Latin American Journal of Solids and Structures
www.lajss.org

# Modeling the size dependent pull-in instability of beam-type NEMS using strain gradient theory

**Abstract**

It is well recognized that size dependency of materials characteristics, i.e. size-effect, often plays a significant role in the performance of nano-structures. Herein, strain gradient continuum theory is employed to investigate the size dependent pull-in instability of beam-type nano-electromechanical systems (NEMS). Two most common types of NEMS i.e. nano-bridge and nano-cantilever are considered. Effects of electrostatic field and dispersion forces i.e. Casimir and van der Waals (vdW) attractions have been considered in the nonlinear governing equations of the systems. Two different solution methods including numerical and Rayleigh-Ritz have been employed to solve the constitutive differential equations of the system. Effect of dispersion forces, the size dependency and the importance of coupling between them on the instability performance are discussed.

**Keywords**

Strain gradient theory, Pull-in instability, Nano-cantilever, Nano-bridge, Dispersion forces, Size effect.

**Ali Koochi**[a]
**Hamid M. Sedighi**[b]
**Mohamadreza Abadyan**[a*]

[a] Shahrekord Branch, Islamic Azad University, Shahrekord, Iran
[b] Department of Mechanical Engineering, Faculty of Engineering, Shahid Chamran University of Ahvaz, Iran

[*]Corresponding Author Email: Abadyan@yahoo.com

## 1 INTRODUCTION

Micro/nano-electromechanical systems (MEMS/NEMS) are increasingly used in various engineering and science branches i.e. mechanics, chemistry, optics, biology, electronics, etc.. Nowadays, these ultra-small systems are utilized in order to develop nano-devices like sensors, actuators, accelerometer, tweezers, switches, etc (Zhang *et al.*, 2004). A beam-type NEMS is constructed from two conductive electrodes, which one of these electrodes is movable and the other one is fixed (grounded). Applying voltage difference between these components causes deflection of the movable one toward the fixed electrode. When the applied voltage exceeds its critical value, which is known as pull-in voltage, the pull-in instability occurs and the movable electrode suddenly adheres to the ground. The electromechanical pull-in instability of microsystems has been investigated by previous researchers during previous decades (Batra *et al.*, 2006; 2008) neglecting nano-scale effects. However,

with decreasing the dimensions to sub-micron, the nano-scale phenomena should be considered in theoretical models. In this paper the effects of two important nano-scale phenomena on the pull-in instability of beam type nano-structures are investigated.

The first phenomenon which appears in nano scale distances is the presence of dispersion forces i.e. Casimir and van der Waals (vdW) force. In distance less than few micrometers, Casimir force significantly affects the nano-beams stability. Casimir force between two plates can be explained via electromagnetic quantum vacuum fluctuations and motion of virtual photons between two conductive surfaces (Lifshitz, 1956) .In recent years, various approaches such as experimental measurements (Buks *et al.*, 2001a; 2001b), using finite element methods (Moghimi Zand *et al.*, 2010;Tadi Beni *et al.*, 2013), experimental observations (Wilson and Beck, 1996; Sundararajan and Bhushan, 2002), applying classic continuum theory (Ramezani *et al.*, 2008; 2007;Farrokhabadi et al., 2013; Tadi Beni *et al.*, 2011), semi-analytical approaches (Noghrehabadi *et al.*, 2011;Koochi and Abadyan 2011; Duan *et al.*, 2013) are utilized to investigate the effect of Casimir force on performance of nano-systems. Another dispersion force that is dominant in nano-scales is the vdW force that affects the stability of nano-structures. If the separation between the interacting bodies is typically less than few nanometers, the retardation effect is negligible and the nano-scale interaction can be modeled as vdW attraction. The pull-in instability of NEMS in the presence of vdW attraction was studied by previous researchers (Kolpekwar *et al.*, 1998; Rotkin, 2002; Lin and Zhao, 2003; Abdi *et al.*, 2011; Soroush *et al.*, 2012; Dequesnes *et al.*, 2002) using various approaches

The second phenomenon in nano-scale is size dependency of the mechanical performance of nano-structures. Experimental observations indicate that elastic characteristics of materials highly are affected by the dimensions and are size dependent (Fleck *et al.*, 1994; Stolken and Evans, 1998). It has been shown that torsional hardening of copper wire increases by a factor of 3 as the wire diameter decreases from 170 to 12 μm (Fleck *et al.* 1994). Stolken and Evans (1998) showed that decrease in thickness of thin nickel beams from 50 to 12.5 μm can lead to great increase in the plastic work hardening of the constitutive material. Other measurements evaluate the material length scale parameter of single crystal and polycrystalline copper to be 12 and 5.84 μm, respectively(McElhaney *et al.*, 1998; Nix and Gao, 1998). Also, the size-dependent behavior has been detected in some kinds of polymers (Chong and Lam, 1999). For hardness measurement of bulk gold, it is found that the plastic length scale parameter (for indentation test and hardness behavior) of Au increases from 470 nm to 1.05 μm with increasing the Au film thickness from 500 nm to 2 μm (Cao *et al.*, 2007). Based on test results gathered via microhardness test, the plastic length scale parameter for metals such as Cu, Ag Brass were determined in the range about 0.2-20 μm based on the crystallity (Al-Rub and Voyiadjis, 2004). Using microbend testing method, the plastic intrinsic material length scale of 4μm for copper and 5μm for nickel were determined (Wang *et al.*, 2003). All these experiments imply that when the characteristic size (thickness, diameter, etc.) of a micro/nano element is in the order of its intrinsic thematerial length scales (typically sub-micron), the material elastic constants highly depend on the element dimensions. The size-dependent behavior of materials and structures at sub-micron distances cannot be modeled using classical continuum mechanics. However, by applying non-classic continuum theories, the size dependent behavior of nano-structures is attributed to material length scale parameters. A length scale parameter might be considered as a mathematical parameter that scales the strain gradients in the constitutive model so

as to balance the dimensions of strains (ε) and strain gradients (dε/dx) (Wang *et al.*, 2003). As the characteristic length of the deformation field becomes significantly larger than the material length scale parameter, strain gradient effects become negligible because the strain terms are much larger than their scaled gradient terms (Wang *et al.*, 2003).

In this regards, the non-classical theories such as non-local elasticity(Eringen and Edelen 1972), couple stress theory (Kong, 2013; Ejike, 1969), strain gradient theory (Lam *et al.*, 2003), modified couple stress theory (Yang *et al.*, 2002) etc. have been developed to consider the size effect in theoretical continuum models. One of the pioneering works in modeling the size-dependent behavior of micro-structures was conducted by Cosserat, in the beginning of 20th century (Cosserat and Cosserat, 1909). Afterwards more general continuum theories have been developed by Toupin (1962), Koiter (1964) and Mindlin (1964) for linear elastic materials in which gradients of normal strains were included and additional material length scale parameters were therefore added as well as Lame constants. The first strain gradient theory was introduced by Mindlin and Eshel (1968) in which the potential energy-density assumed to be depended on the gradient of stain as well as strain. The most comprehensive work was done by Mindlin[14] which contained five additional material parameters and encompassed other non-local theories as special cases Non-local elasticity has been used to study buckling, bending vibration dislocation mechanics, fracture mechanics, surface tension fluids, etc. (Reddy, 2007; Mohammadi *et al*, 2012; 2013; Moosavi *et al*, 2011; Danesh *et al*, 2012; Farajpour *et al*, 2012)

Lam *et al.* (2003), introduced a modified strain gradient theory with three material length scale parameters relevant to dilatation gradient, deviatoric gradient, and symmetric rotation gradient tensors. While some simple size dependent models based on modified couple stress theory have been applied to analyze the pull-in instability of MEMS/NEMS (Tadi Beni *et al.*, 2011; HRokni, *et al.*, 2013; Noghrehabadi *et al.*, 2013; Zhang and Fu, 2012; Mindlin and Tiersten, 1962; Dequesnes *et al.*, 2002; Yin *et al.*, 2011), only rare works have utilized strain gradient theory for analyzing. One of the first works in this field has been conducted by Wang *et al.* (2011a) who modeled the size-dependent instability of clamped structure using strain gradient elasticity theory. However they have not considered the effect of nano-scale attractions such as Casimir and vdW force in their models. In other works (Wang *et al.*, 2011b; 2012) the pull-in instability of rectangular and circular plate MEMS has been investigated. Dynamic pull-in instability and free vibration characteristics of circular microplates subjected to the combined hydrostatic and electrostatic forces are investigated in refs. (Ansari *et al.*, 2013; Mohammadi *et al.*, 2013). However, it should be noted that none of the above mentioned works has taken the important effect of nano-scale forces into account.

In this work, the size-dependent pull-in instability of nano-bridges and nano-cantilevers is investigated considering the effect of vdW and Casimir forces. The strain gradient theory in conjunction with Euler–Bernoulli beam model is used to derive the non-linear equilibrium equation of the systems. The Rayleigh–Ritz method is applied to solve the nonlinear governing equation as well as numerical solution.

## 2. THEORETICAL MODEL

### 2.1. Fundamentals of strain gradient theory

In strain gradient theory in spite of whatever was stated in classic mechanic, equations contain a parameter which introduced as length scale parameter that has statistical nature and indicates that material behavior is depending on material dimensions in micrometer scale. Should be noted that in absence of length scale parameters, the obtained equation of strain gradient theory are turned to the same equations presented in classic mechanic.

Regarding the strain gradient theory modified and suggested by Lam *et al.* (2003), $\bar{U}$ stored strain energy density in the linear elastic and isotropic material with small deformation is written as follows:

$$\bar{U} = \frac{1}{2}\left(\sigma_{ij}\varepsilon_{ij} + p_i\gamma_i + \tau^{(1)}_{ijk}\eta^{(1)}_{ijk} + m^s_{ij}\chi^s_{ij}\right), \tag{1}$$

in which

$$\varepsilon_{ij} = \frac{1}{2}\left(u_{i,j} + u_{j,i}\right) \tag{2}$$

$$\gamma_i = \varepsilon_{mm,i} \tag{3}$$

$$\eta^{(1)}_{ijk} = \frac{1}{3}\left(\varepsilon_{jk,i} + \varepsilon_{ki,j} + \varepsilon_{ij,k}\right) - \frac{1}{15}\delta_{ij}\left(\varepsilon_{mm,k} + 2\varepsilon_{mk,m}\right) - \frac{1}{15}\left[\delta_{jk}\left(\varepsilon_{mm,i} + 2\varepsilon_{mi,m}\right) + \delta_{ki}\left(\varepsilon_{mm,j} + 2\varepsilon_{mj,m}\right)\right] \tag{4}$$

$$\chi^s_{ij} = \frac{1}{2}e_{jkl}u_{l,ki} \tag{5}$$

In above equations, $u_i$, $g_i$, $h^{(1)}_{ijk}$, $c^s_{ij}$, $d_{ij}$ and $e_{ijk}$ indicate components of displacement vector, dilatation gradient vector, deviatoric stretch gradient tensor, symmetric rotation gradient tensor, Kronocker delta and permutation symbol, respectively. Also $s_{ij}$, $p_i$, $t^{(1)}_{ijk}$, $m^s_{ij}$, are components of Cauchy's stress and high order stress tensors, respectively that are identified as the follows (Lam, *et al.*, 2003):

$$\sigma_{ij} = 2\mu\left(\varepsilon_{ij} + \frac{\nu}{1-2\nu}\varepsilon_{mm}\delta_{ij}\right) \tag{6}$$

$$p_i = 2\mu l_0^2\gamma_i \tag{7}$$

$$\tau^{(1)}_{ijk} = 2\mu l_1^2\eta^{(1)}_{ijk} \tag{8}$$

$$m^s_{ij} = 2\mu l_2^2\chi^s_{ij} \tag{9}$$

In the above equations, ν and μ are Poisson's ratio and shear modulus, respectively. Also $l_0$, $l_1$and $l_2$ are additional material length scale parameters those which are depending on dilatation gradient vector, deviatoric stretch gradient tensor and symmetric rotation gradient tensor.

## 2.2. Nonlinear constitutive equation

Figures (1a) and (1b) show schematic representation of beam-type nano-cantilever and double clamped nano-beam (nano-bridge) that is applied in electromechanical structures such as actuators, respectively. Herein, the nano-structures with a beam length of L, wide of b and thickness of h are considered.

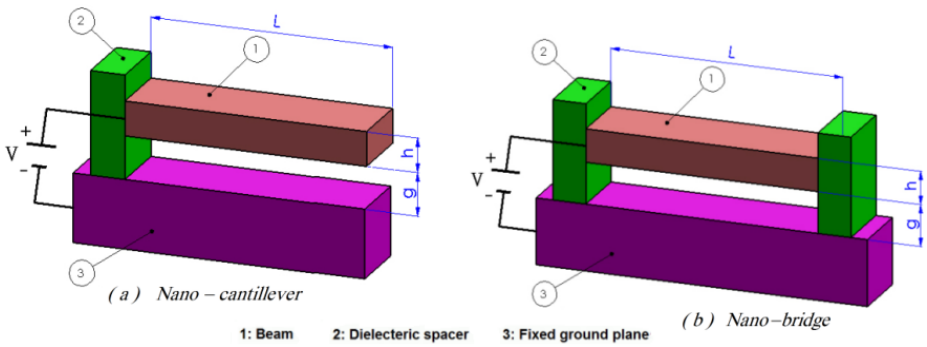


**Figure 1:** Schematic representations of (a) nano-cantilever and (b) nano-bridge.

### 2.2.1. Strain energy

The total strain energy, U, for a deformed Euler–Bernoulli beam is given by:

$$U = U_{bending} + U_{stretching} \tag{10}$$

where, $U_{stretching}$ and $U_{bending}$ are energy stored in the beam due to axial forces and bending strain, respectively.

In this work, the displacement field of Euler-Bernoulli beam theory is applied for modeling the elastic behavior of the nano-structures. Based on this theory, the displacement field can be written as the following:

$$u_1 = -Z\frac{\partial W}{\partial X} \quad u_2 = 0 \quad u_3 = W(X) \tag{11}$$

The variable, W, indicates beam displacement in direction of Z axis. Substituting the linear displacement field of equation (11) in equations (1)-(9), after some elaborations the bending strain energy is obtained as the following

$$U_{bending} = \int_V \bar{U}\, dV = \frac{1}{2}\int_0^L \left[ \left( EI + 2\mu A l_0^2 + \frac{8}{15}\mu A l_1^2 + \mu A l_2^2 \right) \left( \frac{d^2W}{dX^2} \right)^2 + A\left( 2\mu l_0^2 + \frac{4}{5}\mu l_1^2 \right) \left( \frac{d^3W}{dX^3} \right)^2 \right] dX \tag{12}$$

In above equation, I is the second cross section moment around Y axis.
Now, the stretching energy stored in the beam due to axial forces can be written as

$$U_{stretching} = \frac{1}{2}\int_0^L F_a \left( \frac{dW}{dX} \right)^2 dX \tag{13}$$

In the above equation, $F_a$ is the axial resultant force associated with the mid-plane stretching (in the absence of external axial force, thermal stress, etc.). Note that there is no axial stretching ($F_a$=0) for nano-cantilever due to the movability of the free end and therefore the amount of energy $U_{stretching}$ equals zero. In the case of nano-bridge, axial force associated with the mid-plane stretching ($F_a$) should be contributed in the total energy. When nano-beam is in tension, the actual beam length $L'$ will become longer than the original length L. However, the beam is immovable in the Z- and X-directions at both ends of the nano-bridge. Thus, an additional axial force will occur and can be expressed as:

$$F_a = \frac{EA}{L}\left(L' - L\right) = \frac{EA}{2L}\int_0^L \left(\frac{dW}{\partial X}\right)^2 dX \tag{14}$$

### 2.2.2. Work of external forces

Considering the distribution of external forces per unit length of the beam ($f_{external}$), the work by these external forces can be obtained as:

$$V_{external} = \int_0^L f_{external} W(X) dX \tag{15}$$

Now, by Considering the first order fringing field correctness effect the electrostatic force per unit length of the beam is written as the following (Ramezani *et al.*, 2008):

$$f_{elec} = \frac{\varepsilon_0 b V^2}{2\left(g - W(X)\right)^2}\left(1 + 0.65\frac{\left(g - W(X)\right)}{b}\right) \tag{16}$$

In the above equation $\varepsilon_0$= $8.854\times10^{-12}$ $c^2$ $N^{-1}m^{-2}$ is the permittivity of vacuum. V is external voltage applied to nano-actuator and g is initial distance between ground and movable electrodes.

The dispersion forces per unit length of the beam ($f_{disp}$) are defined considering the van der Waals and Casimir forces. Based on what is mentioned in section 1, two interaction regimes can be defined: first, the large separation regime in which the Casimir force is dominant (typically above several tens of nanometers (Israelachvili and Tabor, 1972; Klimchitskaya *et al.*, 2000; Bostrom and Sernelius, 2000)). Considering the ideal case, the Casimir interaction is proportional to the inverse fourth power of the separation (Gusso and Delben, 2008):

$$f_{Cas} = \frac{\pi^2 \hbar c b}{240\left(g - W\left(X\right)\right)^4} \tag{17}$$

where $\hbar$=$1.055\times10^{-34}\,Js$ is Planck's constant divided by 2π and c=2.998×10^8 m/s is the light speed.

The second regime is the small separation regime (typically below several tens of nanometers (Israelachvili and Tabor, 1972; Klimchitskaya *et al.*, 2000; Bostrom and Sernelius, 2000)), in which the van der Waals force is the dominant attraction. In this case, the attraction between two ideal surfaces is proportional to the inverse cube of the separation:

$$f_{vdW} = \frac{\bar{A}b}{6\pi(g - W(X))^3} \tag{18}$$

where $\bar{A}$ is the Hamaker constant.
Finally total energy of system can be summarized as:

$$\begin{aligned}\Pi = &\frac{1}{2}\int_0^L \left[\left(EI + 2\mu A l_0^2 + \frac{8}{15}\mu A l_1^2 + \mu A l_2^2\right)\left(\frac{d^2W}{dX^2}\right)^2 + A\left(2\mu l_0^2 + \frac{4}{5}\mu l_1^2\right)\left(\frac{d^3W}{dX^3}\right)^2\right]dX \\ &+\frac{1}{2}\int_0^L F_a\left(\frac{dW}{dX}\right)^2 dX - \int_0^L f_{external} W(X)dX\end{aligned} \tag{19}$$

Now, by using the substitutions x=X/L and w=W/g the nondimentional total energy can be explained as:

$$\begin{aligned}\bar{\Pi} = &\frac{1}{2}\int_0^1 \left[\left(1 + \frac{\mu_s}{15}\left(30\left(\frac{l_0}{l_2}\right)^2 + 8\left(\frac{l_1}{l_2}\right)^2 + 15\right)\right)\left(\frac{d^2w}{dx^2}\right)^2 + \frac{\mu_s}{30(\lambda)^2}\left(5\left(\frac{l_0}{l_2}\right)^2 + 2\left(\frac{l_1}{l_2}\right)^2\right)\left(\frac{d^3w}{dx^3}\right)^2\right]dx \\ &+\frac{1}{2}\int_0^1 \eta\left[\int_0^1 \left(\frac{dw}{dx}\right)^2 dx\right]\left(\frac{dw}{dx}\right)^2 dx - \int_0^L \left(\frac{\alpha_n}{(1-w)^n} + \frac{\beta^2}{(1-w)^2}(1 + 0.65\gamma(1-w))\right)w(\mathrm{x})dx\end{aligned} \tag{20}$$

where the dimensionless parameters are identified as:

$$\alpha_n = \begin{cases} \dfrac{\bar{A}bL^4}{6\pi g^4 EI} & \text{vdW interaction } (n = 3) \\ \dfrac{\pi^2 \hbar c b L^4}{240 g^5 EI} & \text{Casimir interaction } (n = 4) \end{cases} \tag{21a}$$

$$\beta = V\sqrt{\frac{\varepsilon_0 bL^4}{2g^3 EI}} \tag{21b}$$

$$\gamma = \frac{g}{b} \tag{21c}$$

$$\mu_s = \frac{12\mu}{E(h/l_2)^2} \tag{21d}$$

$$\lambda = \frac{L}{h} \tag{21e}$$

$$\eta = \begin{cases} 6\left(\dfrac{g}{h}\right)^2 & \text{nano-bridge} \\ 0 & \text{nano-cantilever} \end{cases} \tag{21f}$$

In above relations, $\beta$, $\mu_s$ and $\alpha_n$ interpret the dimensionless values of applied voltage, size-effect and dispersion forces.

## 3. SOLUTION METHODS

### 3.1. Rayleigh–Ritz method

To solve the governing equation of the systems, the displacement is expressed as a linear combination of a complete set of linearly independent basis functions $\varphi_i(x)$ in the form of:

$$w(x) = \sum_{i=1}^{n} q_i \phi_i(x) \tag{22}$$

where the index i refers to the number of modes included in the simulation. We use the linear mode shapes of the nano-beam (based on classic continuum theory) as basic functions in the Rayleigh–Ritz procedure. The classic mode shapes of cantilever nano-beam can be expressed as:

$$\phi_i(\xi) = \cosh(\lambda_i\xi) - \cos(\lambda_i\xi) - \frac{\cosh(\lambda_i) - \cos(\lambda_i)}{\sinh(\lambda_i) - \sin(\lambda_i)}\left(\sinh(\lambda_i\xi) - \sin(\lambda_i\xi)\right) \tag{23}$$

where $\lambda_i$ is the $i^{th}$ root of characteristic equation of clamped-free (for nano-cantilever) or clamped-clamped (for nano-bridge) beams. Considering the equilibrium of the system, one can write:

$$\frac{\partial \bar{\Pi}}{\partial q_i} = 0 \quad i = 0,1,...,N \tag{24}$$

This led to a system of algebraic equation which can be solved numerically to obtain the final solution. Using Taylor expansion for electrostatic and dispersion force, substituting (20) and (22) into (24), assuming the orthogonality of $\varphi_i(x)$ and then following some straightforward mathematical elaborations a system of algebraic equation can be fined as:

$$\begin{aligned}
&\left[1+\frac{\mu_s}{15}\left(30\left(\frac{l_0}{l_2}\right)^2+8\left(\frac{l_1}{l_2}\right)^2+15\right)\right]\lambda_i^4 q_i - \frac{\mu_s}{30(\lambda)^2}\left[5\left(\frac{l_0}{l_2}\right)^2+2\left(\frac{l_1}{l_2}\right)^2\right]\int_0^1 \phi_i \sum_{j=1}^{N} q_j \frac{d^6\phi_j}{dx^6}dx \\
&-\eta\int_0^1 \phi_i \left\{\left[\int_0^1 \left(\sum_{j=1}^{N} q_j \frac{d\phi_j}{dx}\right)^2 dx\right]\sum_{j=1}^{N} q_j \frac{d^2\phi_j}{dx^2}\right\}dx - \int_0^1 \phi_i \sum_{k=0}^{\infty} A_k \left(\sum_{j=1}^{N} q_j\phi_j\right)^k dx + B.C. = 0 \\
&\qquad\qquad\qquad\qquad\qquad\qquad\qquad\qquad\qquad\qquad\qquad\qquad\qquad\qquad\qquad\qquad i = 1,2,..,N
\end{aligned} \tag{25}$$

where N is the number of considered terms of Rayleigh–Ritz and $A_k$ is the Taylor expansion coefficient of electrostatic and dispersion force. In above equation, the boundary condition terms, B.C., is defined as:

$$
\begin{aligned}
B.C. = & \frac{\mu_s}{30(\lambda)^2}\left(5\left(\frac{l_0}{l_2}\right)^2+2\left(\frac{l_1}{l_2}\right)^2\right)\left(\sum_{j=1}^{N} q_j \frac{d^3}{dX^3}\phi_j\right)\frac{d^2\phi_i}{dX^2}\Bigg|_{x=1} \\
& -\frac{\mu_s}{30(\lambda)^2}\left(5\left(\frac{l_0}{l_2}\right)^2+2\left(\frac{l_1}{l_2}\right)^2\right)\left(\sum_{j=1}^{N} q_j \frac{d^3}{dX^3}\phi_j\right)\frac{d^2\phi_i}{dX^2}\Bigg|_{x=0} \\
& +\frac{\mu_s}{30(\lambda)^2}\left(5\left(\frac{l_0}{l_2}\right)^2+2\left(\frac{l_1}{l_2}\right)^2\right)\left(\sum_{j=1}^{N} q_j \frac{d^5}{dX^5}\phi_j\right)\phi_i\Bigg|_{x=1} \\
& -\frac{\mu_s}{30(\lambda)^2}\left(5\left(\frac{l_0}{l_2}\right)^2+2\left(\frac{l_1}{l_2}\right)^2\right)\left(\sum_{j=1}^{N} q_j \frac{d^4}{dX^4}\phi_j\right)\frac{d\phi_i}{dX}\Bigg|_{x=1}
\end{aligned}
\tag{26}
$$

for nano-cantilever and:

$$
\begin{aligned}
B.C. = & \frac{\mu_s}{30(\lambda)^2}\left(5\left(\frac{l_0}{l_2}\right)^2+2\left(\frac{l_1}{l_2}\right)^2\right)\frac{d^3}{dX^3}\left(\sum_{j=1}^{N} q_j\phi_j\right)\frac{d^2\phi_i}{dX^2}\Bigg|_{x=1} \\
& -\frac{\mu_s}{30(\lambda)^2}\left(5\left(\frac{l_0}{l_2}\right)^2+2\left(\frac{l_1}{l_2}\right)^2\right)\frac{d^3}{dX^3}\left(\sum_{j=1}^{N} q_j\phi_j\right)\frac{d^2\phi_i}{dX^2}\Bigg|_{x=0}
\end{aligned}
\tag{27}
$$

for nano-bridge.

The Maple commercial software is employed to numerically solve the system of algebraic equations.

### 3.2. Numerical method

In addition with the Rayleigh–Ritz method, the deflection of the nano-structures is numerically simulated and the results are compared with those of Rayleigh–Ritz method. Utilizing Hamilton principle i.e. $\delta\left(\bar{\Pi}\right)=0$, in which δ indicates variations symbol, the governing equation of lateral deflection of the system can be derived as the following

$$
\begin{aligned}
& \left[1+\frac{\mu_s}{15}\left(30\left(\frac{l_0}{l_2}\right)^2+8\left(\frac{l_1}{l_2}\right)^2+15\right)\right]\frac{\partial^4 w}{\partial x^4}-\frac{\mu_s}{30(\lambda)^2}\left(5\left(\frac{l_0}{l_2}\right)^2+2\left(\frac{l_1}{l_2}\right)^2\right)\frac{\partial^6 w}{\partial x^6}= \\
& \frac{\alpha_n}{(1-w)^n}+\frac{\beta^2}{(1-w)^2}(1+0.65\gamma(1-w))
\end{aligned}
\tag{28}
$$

following boundary conditions of nano- cantilever is:

$$\begin{aligned}
&w(0)=\frac{dw}{dx}(0)=\frac{d^3w}{dx^3}(0)=0\\
&\left[1+\frac{\mu_s}{15}\left(30\left(\frac{l_0}{l_2}\right)^2+8\left(\frac{l_1}{l_2}\right)^2+15\right)\right]\frac{d^3w}{dx^3}(1)-\frac{\mu_s}{30(\lambda)^2}\left(5\left(\frac{l_0}{l_2}\right)^2+2\left(\frac{l_1}{l_2}\right)^2\right)\frac{d^5w}{dx^5}(1)=0\\
&\left[1+\frac{\mu_s}{15}\left(30\left(\frac{l_0}{l_2}\right)^2+8\left(\frac{l_1}{l_2}\right)^2+15\right)\right]\frac{d^2w}{dx^2}(1)-\frac{\mu_s}{30(\lambda)^2}\left(5\left(\frac{l_0}{l_2}\right)^2+2\left(\frac{l_1}{l_2}\right)^2\right)\frac{d^4w}{dx^4}(1)=0\\
&\frac{d^3w}{dx^3}(1)=0
\end{aligned} \tag{29}$$

Similarly for nano-bridge by using Eq. 21 the governing equation is obtained as:

$$\begin{aligned}
&\left[1+\frac{\mu_s}{15}\left(30\left(\frac{l_0}{l_2}\right)^2+8\left(\frac{l_1}{l_2}\right)^2+15\right)\right]\frac{\partial^4w}{\partial x^4}-\frac{\mu_s}{30(\lambda)^2}\left(5\left(\frac{l_0}{l_2}\right)^2+2\left(\frac{l_1}{l_2}\right)^2\right)\frac{\partial^6w}{\partial x^6}-\eta\left[\int_0^1\left(\frac{\partial w}{\partial x}\right)^2dx\right]\frac{d^2w}{dx^2}=\\
&\frac{\alpha_n}{(1-w)^n}+\frac{\beta^2}{(1-w)^2}(1+0.65\gamma(1-w))
\end{aligned} \tag{30}$$

And the following boundary conditions

$$\begin{aligned}
&w(0)=\frac{dw}{dX}(0)=\frac{d^3w}{dX^3}(0)=0\\
&w(1)=\frac{dw}{dX}(1)=\frac{d^3w}{dX^3}(1)=0
\end{aligned} \tag{31}$$

The nonlinear governing differential equation is solved with the boundary value problem solver of MAPLE commercial software (For nano-bridge, an iterative procedure is required to solve the integro-differential equation). The step size of the parameter variation is chosen based on the sensitivity of the parameter to the maximum deflection (tip deflection for nano-cantilever and mid-length deflection for nano-bridge. The pull-in parameters are determined via the slope of the w-β graphs.
It should be noted that the governing equation of the structures based on the classical theory is achieved by setting the $l_0$, $l_1$ and $l_2$ equal to zero. In addition, the size-dependent behavior of nano-beam based on the modified couple stress theory can be obtained by considering $l_0$=$l_1$=0 and $l_2$=l (Rajabi and Ramezani, 2013).

### 3.3. Validation

To validate the Rayleigh–Ritz method and check the convergence rate of series, effect of increasing the number of modes on the pull-in deflection and voltage of a typical cantilever nano-actuator with $\alpha_n$=0.5, $\gamma$=0.4, $h/l_2$=3, $\lambda$=20 and $l_0=l_1=l_1$ are presented in Table 1. This table reveals the convergence of the series with increasing the number of modes. By selecting three modes, an acceptable error is achieved.

| | Rayleigh–Ritz Method | | | Numerical |
|---|---|---|---|---|
| | 1 Term | 2 Terms | 3 Terms | |
| $\beta_{PI}$ | 1.97 | 2.03 | 2.04 | 2.05 |
| Error(%) | -3.90 | -0.98 | -0.48 | - |
| $w_{PI}(x=1)$ | 0.4565 | 0.4384 | 0.4336 | 0.4305 |
| Error(%) | 6.039 | 1.835 | 0.720 | - |

**Table 1:** The convergence check of Rayleigh–Ritz

## 4. RESULT AND DISCUSSION

A typical nano-actuator with the geometrical characteristics of $\eta$=24, g/h=2, $\lambda$=25 and $\gamma$=g/b=0.1 are considered. The Young's modulus E, and shear modulus $\mu$ are 169 GPa and 65.8 GPa, respectively.

### 4.1. NEMS deflection and pull-in instability

Figures 2 and 3 show the variation of deflection of a typical nano-cantilever and nano-bridge, respectively, when the applied voltage increases from zero to pull-in value. In these figures, the vertical axes reveal the deflection of the nano-beams while the horizontal axes reveal the dimensionless length of the beams.

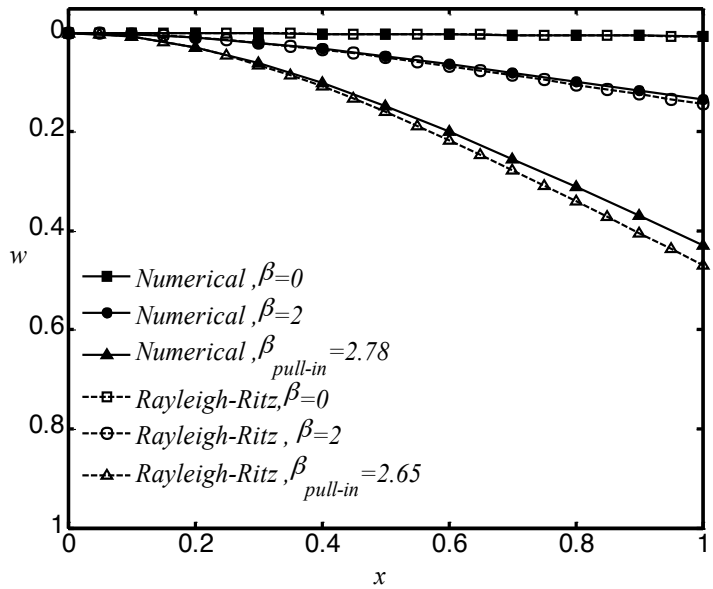


**Figure 2:** Deflection of typical nano-cantilever for different values of applied voltage from zeroto pull in voltage considering the Casimirforce ( $a_4 = 0.25$).

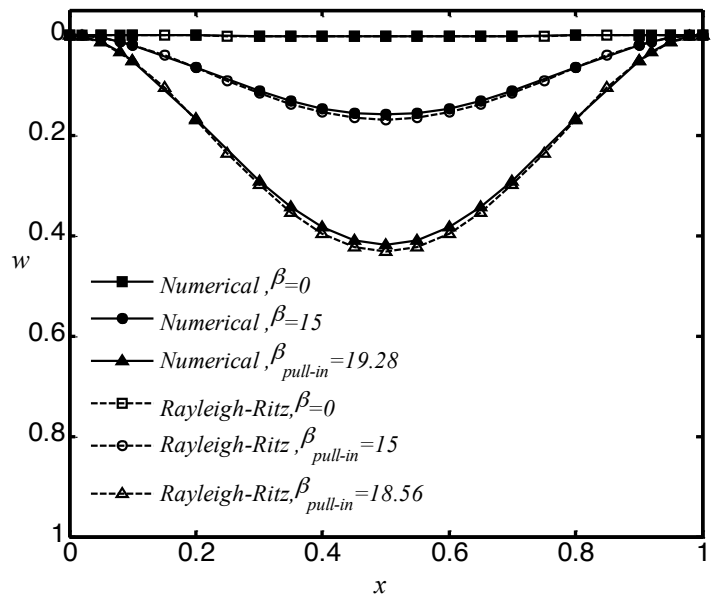


**Figure 3:** Deflection of typical nano-bridge for different values of applied voltage from zero to pull-in voltage considering vdW force ( $a_3 = 5$).

The dimensionless material length scale parameters $l_0/l_2$, $l_1/l_2$ and $h/l_2$ values for both nano-structures are selected as 1, 1 and 2, respectively. As seen, increasing the applied voltage increase the deflection of the nano-beams. When the applied voltage exceeds its critical value, $\beta_{PI}$, then no solution exists and the pull-in instability occurs. From the mathematical point of view, the instabil-

ity occurs when $dw(x = 1)/db^2 \text{Æ } 0$ for nano-cantilever and $dw(x = 0.5)/db^2 \text{Æ } 0$ for nano-bridge. The instability parameters of the system can be determined via the slope of the w-β graphs by plotting w vs.β.

Note that the operation distance of the nano-systems is limited by the pull-in instability. It is shown that the results of Rayleigh–Ritz method are in good agreement with those of numerical method. The relative error of presented methods with respect to the numerical solution is within the acceptable range for most engineering applications.

## 4.2. Influence of size effect

Figures 4 and 5 show the variation of normalized maximum tip deflection of the structures when the applied voltage increases from zero to pull-in value. Figure 4 corresponds to typical nano-cantilever operated in Casimir regime ($\alpha_4$=0.25) and Figure 5 corresponds to a nano-bridge operated in vdW regime ($\alpha_3$=5).The results are calculated using three different theories i.e. size-independent classical theory ($l_0$=$l_1$=$l_2$=0), the modified couple stress theory ($l_0$=$l_1$=0 and $l_2$=l) and strain gradient theory. The thickness of the nano-beams is selected twice of length scale parameter (h/l=2). These figures reveal that for a given applied voltage, the deflection value determined by classic theory is greater than those predicted by strain gradient theory and modified couple stress theory. In other word, size effect results in a hardening behavior of the structures. These figures demonstrate that in the strain gradient theory, the hardening effect of $l_0$ is more pronounced than $l_1$.

Figures 4and 5 also reveal that the nano-beam has an initial deflection due to the presence of attractive dispersion forces even, when no voltage is applied (β=0).

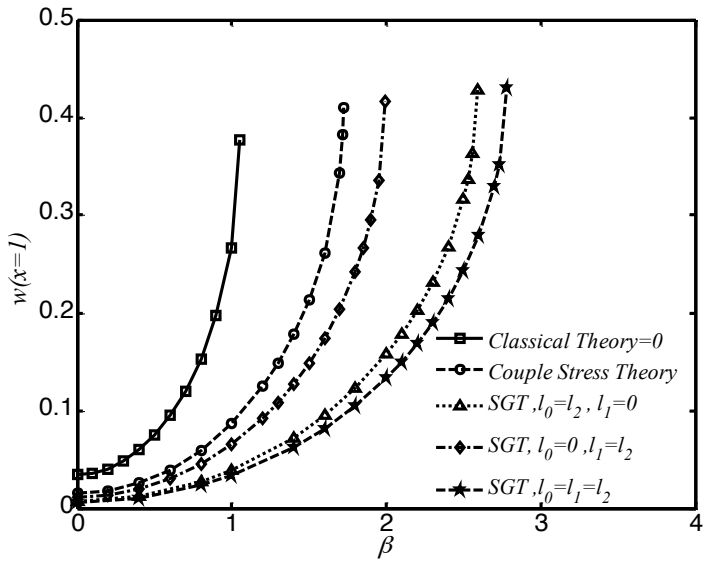


(a)

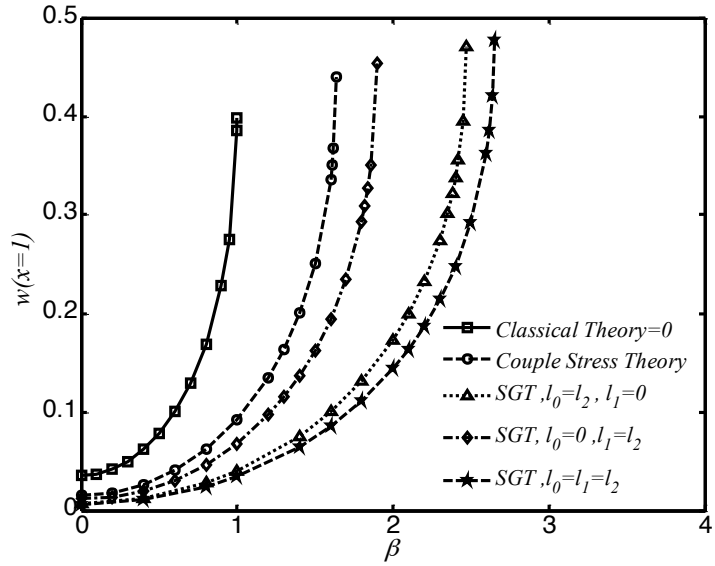


(b)

**Figure 4:** The variation of nano-cantilever tip displacement versus applied voltage parameter (Casimirregime: $a_4 = 0.25$) determined via different continuum theories(a) Numerical (b) Rayleigh-Ritz

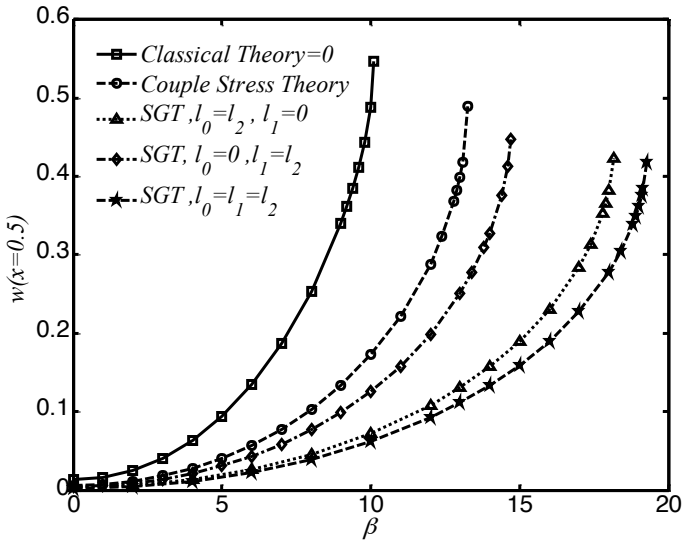


(a)

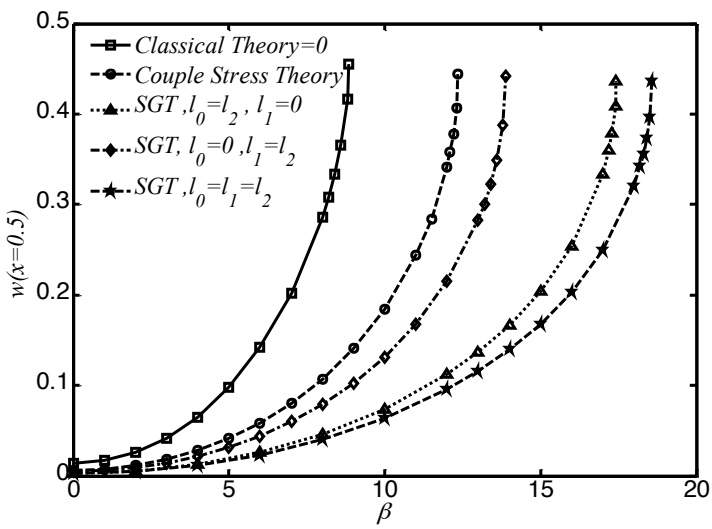


(b)

**Figure 5:** The variation of nano-bridge mid-length displacement versus applied voltage parameter (vdW regime: $a_3 = 5$) determined via different continuum theories: (a) Numerical (b) Rayleigh-Ritz

### 4.3. Coupling between size effect and dispersion forces

In nano-scale, both dispersion forces and size effect are significant. Variation of the pull-in voltage ($\beta_{PI}$) of the nano-beams is demonstrated in Figures 6 and 7 as a function of the nano-scale parameter ($h/l_2$). Figure 6 presents the results for nano-cantilever that operates in Casimir regime and Figure 7 corresponds to the nano-bridge operates in vdW regime. The horizontal lines correspond to the pull-in voltage ($\beta_{PI}$) when no size effect has been considered (i.e. classical theory). These figures

show that dispersion forces decrease the pull-in voltage of system. Moreover, without considering dispersion force ($\alpha_n$=0), decreasing $h/l_2$ results in decreasing the $\beta_{PI}$ of nano-systems. It should be noted that decrease in $h/l_2$ value corresponds to increase in size effect. This means size effect provides a hardening behavior that enhances the elastic resistance and consequent pull-in voltage of the nano-devices. On the other hand, with increase in the beam thickness, results of strain gradient theory approaches to those of classic continuum theory i.e. enhancing the beam thickness decreases the size-effect. This trend is also observed in the presence of dispersion forces where the pull-in voltage increases with increasing the size-effect.

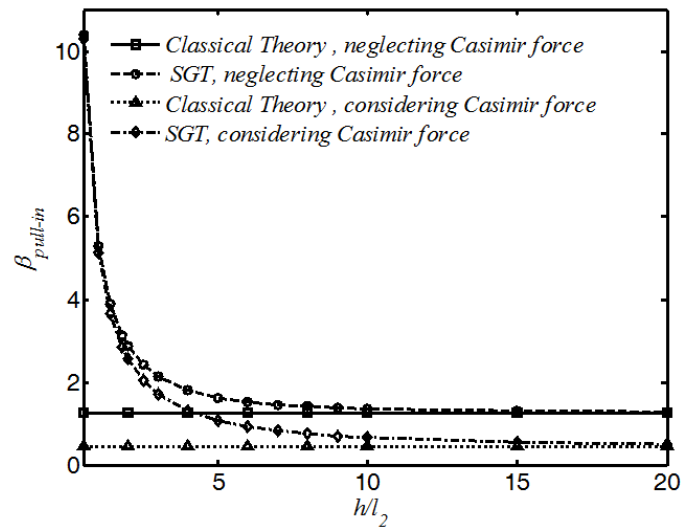


(a)

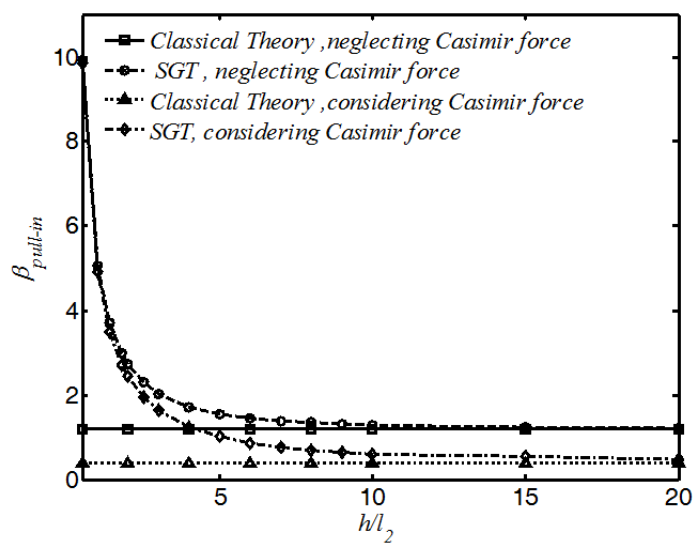


(b)

**Figure 6:** Influence of Size effect on pull-in voltage ofnano-Cantilever considering Casimir regime ( $a_4 = 0.8$)(a) Numerical (b) Rayleigh-Ritz

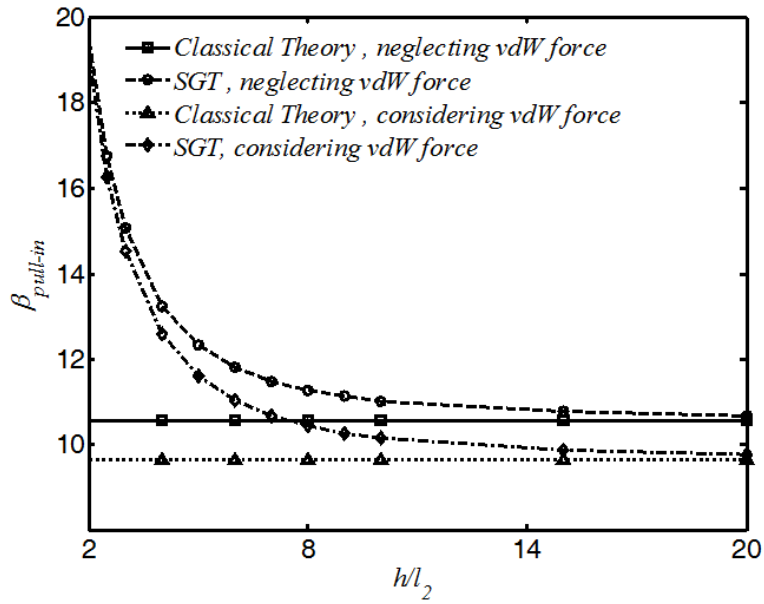


(a)

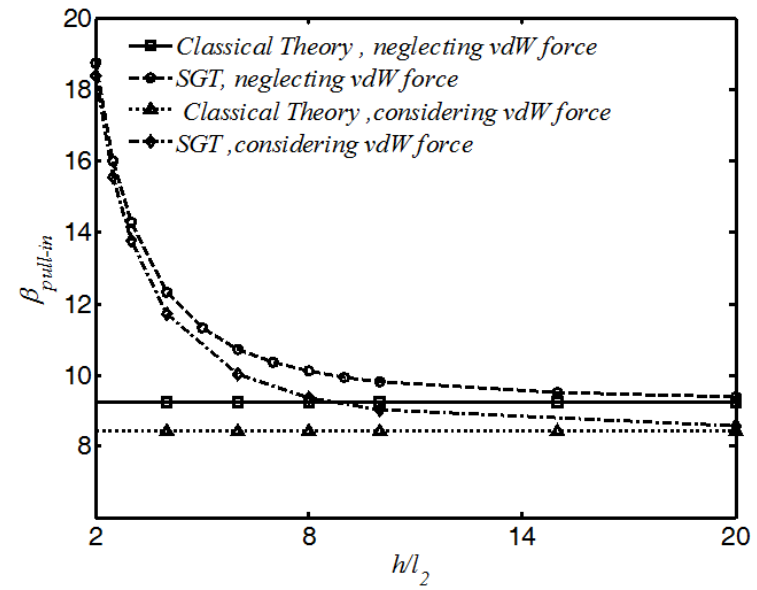


(b)

**Figure 7:** Influence of Size effect on pull-in voltage ofnano-bridge considering vdW regime ( $a_3 = 10$ ). (a) Numerical (b) Rayleigh-Ritz.

Figures 8 and 9 represent the influence of size effect ($h/l_2$) on the instability deflection ($w_{PI}$) of the nano-cantilever and nano-bridge, respectively. Figure 8 shows that in the absence of dispersion force ($\alpha_4$=0), the pull-in deflection of nano-cantilever is independent of length scale parameter ($h/l_2$). However, as seen from figure 9 in the absence of dispersion force ($\alpha_3$=0), the pull-in deflection of a nano-bridge decreases by increasing the size effect. This difference is the result of stretching that induces non-linearity in governing differential equation of nano-bridge. Moreover, as seen in figures

8, the pull-in deflection of nano-cantilever in the presence of dispersion force increases with increase in size effect Note that this trend is different from what observed for nano-bridge in the presence of dispersion force ($\alpha_3$=10), where $w_{PI}$ decreases with increasing in size effect.

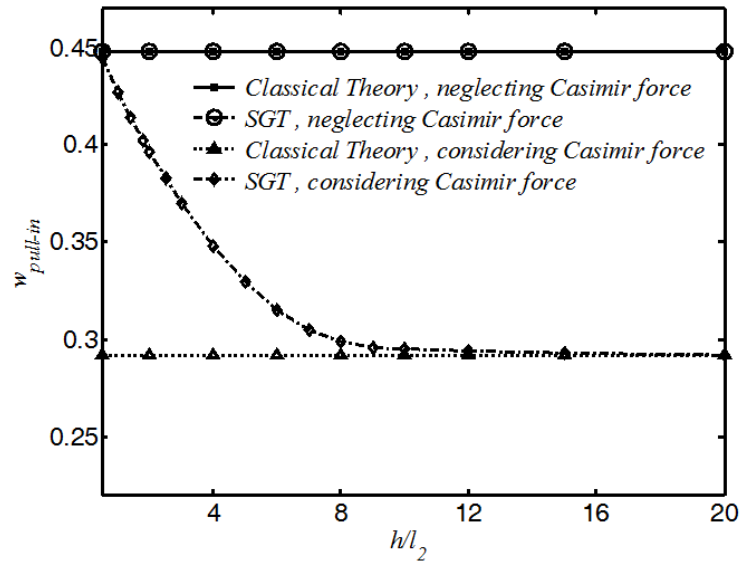


(a)

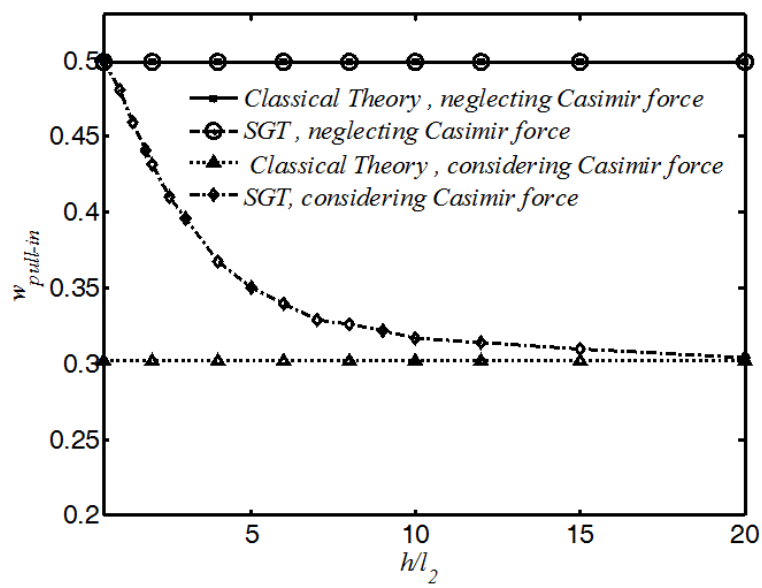


(b)

**Figure 8:** Influence of Size effect on the pull-in deflection ofnano-cantilever operated in Casimir regime ($a_4 = 0.8$). (a) Numerical (b) Rayleigh-Ritz

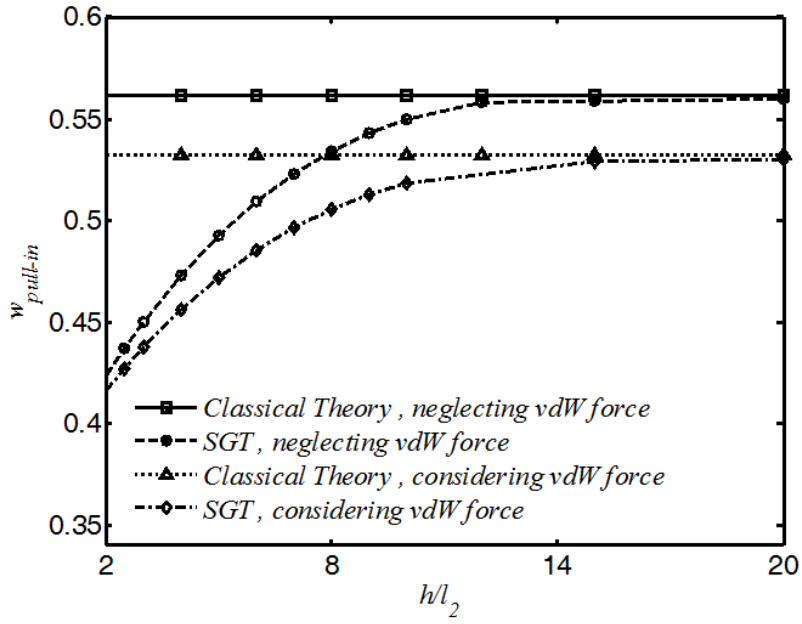


(a)

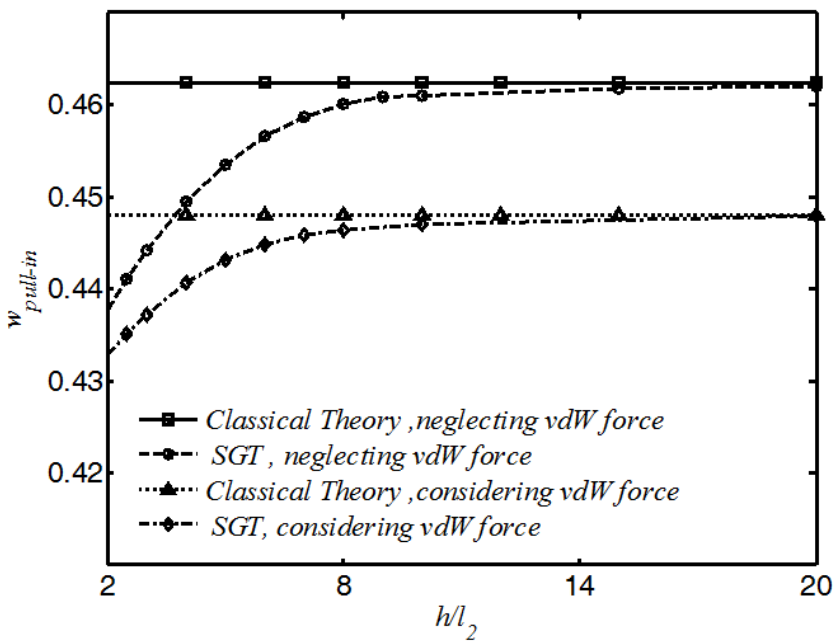


(b)

**Figure 9:** Influence of Size effect on the pull-in deflection ofnano-bridge operated in vdW regime ( $a_3 = 10$ ). (a) Numerical (b) Rayleigh-Ritz

### 4.4. Comparison with literature

To evaluate the model and compare with the literature, the deflection-voltage graphs for typical nano-structures have been simulated in this subsection. The geometrical characteristics of the nano-actuator i.e. width, thickness and initial gap are 8000, 340 and 1019 nm, respectively (Sadeghian *et al.*, 2009). Furthermore, the Young's modulus E and Poison's ratio ν are 169 GPa and 0.064, respectively ((Sadeghian *et al.*, 2009). Figures 10 compares the pull-in voltages evaluated by the modified strain gradient theory with the results of the classical theory and also the experimental observations reported by Sadeghian *et al.* (2009) for nano-cantilever. With $l = 38$ nm, the best fit for the modified strain gradient theory and the experimental results is achieved for the considered beams. As seen, the strain gradient is reliable to predict pull-in voltage of electromechanical systems. Results of present study show that the coupling of size effect and dispersion force is a crucial issue to precise determining the pull-in parameters of the nano-structures and should be included in theoretical models.

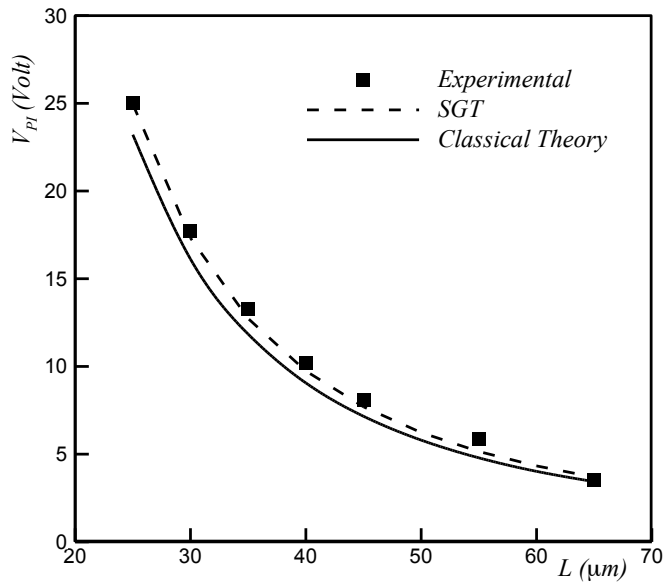


**Figure 10:** Comparison between experimental (Sadeghian et al., 2009) measurements with predictions of classical continuum and strain gradient theory for cantilever MEMS.

## 5. CONCLUSION

In this article, strain gradient theory has been employed to investigate the influence of size-effect on pull-in performance of nano-beams, incorporating the effect of dispersion force. The nonlinear governing equation was solved using two different approaches, i.e. Rayleigh-Ritz method and numerical solution. Comparison between solving methods reveals that Rayleigh-Ritz method is in good agreement with numerical solution. It is found that:

- The presence of dispersion force reduces the pull-in voltage of the system. This nano-scale force induces an initial deflection in freestanding nano-structures and reduces the pull-in deflection of the nano-bridges and nano-cantilevers.
- Size-effect provides a stiffness behavior on electromechanical response of the nano- devices. The size effect increases the pull-in voltage of nano-actuator due to the stiffness effect.
- In small sizes of beam thickness, as this size can be compared with material length size, there are a substantial difference between the results of classic continuum theory and those of strain gradient and modified couple stress theories.
- In absence of vdW force in nano-bridge, the pull-in voltage increases but deflection decreases with increase in size effect. While for nano-cantilever in absence of Casimir force, pull-in voltage increases but deflection does not change with increase in size effect parameter.
- In the presence of dispersion forces, pull-in voltage of the nano-bridge increases with increasing the size effect. Interestingly, increasing the size effect decreases the pull-in deflection of the nano-bridge. However, for nano-cantilever (in the presence of dispersion force), both pull-in voltage and deflection increase with increase in size effect parameter.

## References

Abdi, J., Koochi, A., Kazemi, A. S., Abadyan, M. (2011) Modeling the effects of size dependency and dispersion forces on the pull-in instability of electrostatic cantilever NEMS using modified couple stress theory. Smart Materials and Structures 20: 055011 (9 pp).

Al-Rub, R. K. A., and Voyiadjis, G. Z. (2004) Determination of the Material Intrinsic Length Scale of Gradient Plasticity Theory. Int. J. Multiscale Comput. Eng. 2(3):377-400.

Ansari, R., Gholami, R., Mohammadi, V., Faghih Shojaei, M. (2013) Size-Dependent Pull-In

Batra, R.C., Porfiri, M., Spinello, D. (2006) Capacitance estimate for electrostatically actuated narrow microbeams, Micro and Nano Letters 1:71–73.

Batra, R.C., Porfiri, M., Spinello, D. (2008) Reduced-order models for microelectromechanical rectangular and circular plates incorporating the Casimir force. International Journal of Solids and Structures 45:3558–3583.

Bostrom, M. and Sernelius, B. E. (2000) Fractional van der Waals interaction between thin metallic films. Physical Review B 61:2204-2210

Buks, E., and Roukes, M.L. (2001) Metastability and the Casimir effect in micromechanical systems. Europhysics Letters 54:220–226.

Buks, E., and Roukes, M.L. (2001) Stiction, adhesion energy, and the Casimir effect in micromechanical systems. Physical Review B 63:033402.

Cao, Y., Nankivil, D. D., Allameh, S., Soboyejo W. O. (2007) Mechanical Properties of Au Films on Silicon Substrates. Mater. Manuf. Process 22: 187–194,

Chong, A.C.M. and Lam, D.C.C. 1999. Strain gradient plasticity effect in indentation hardness of polymers. J. Mater. Res. 14(10):4103-4110

Cosserat, E., Cosserat, F. (1909) Theorie des Corps Deformables, Hermann et Fils, Paris.

Danesh M., Farajpour A., Mohammadi M. (2012) Axial vibration analysis of a tapered nanorod based on nonlocal elasticity theory and differential quadrature method, Mechanics Research Communications 39: 23– 27.

Dequesnes, M., Rotkin, S. V., Aluru, N. R. (2002) Calculation of pull-in voltages for carbon nanotube-based nanoelectromechanical switches, Nanotechnology 13 :120–131.

Dequesnes, M., Rotkin, S. V., Aluru, N. R. (2002) Calculation of Pull-in Voltage for Carbon-Nanotube-Based Nanoelectromechanical Switches. Nanotechnology 13: 120–131.

Duan, J. S. , Rach, R., Wazwaz, A. M. (2013) Solution of the model of beam-type micro- and nano-scale electrostatic actuators by a new modified Adomian decomposition method for nonlinear boundary value problems. International Journal of Non-Linear Mechanics 49:159–169

Ejike U.B.C.O. (1969) The plane circular crack problem in the linearized couple-stress theory, International Journal of Engineering Science 7:947–961.

Eringen, A.C. and Edelen D.B.G. (1972) On nonlocal elasticity" International Journal of Engineering Science 10:233–248.

Farajpour A., Shahidi A. R., Mohammadi M., Mahzoon M. (2012) Buckling of orthotropic micro/nanoscale plates under linearly varying in-plane load via nonlocal continuum mechanics, Composite Structures 94:1605–1615.

Farrokhabadi, A., Koochi, A., Abadyan, M. (2013) Modeling the instability of CNT tweezers using a continuum model. Microsystem Technologies 1-12. DOI: 10.1007/s00542-013-1863-3

Fleck, N. A., Muller, G. M., Ashby, M. F., Hutchinson, J. W. (1994) Strain gradient plasticity: theory and experiment. Acta Metallurgica et Materialia 42:475-487.

Gusso, A. and Delben, G. J. (2008) Dispersion force for materials relevant for micro- and nanodevices fabrication. Journal of Physics D: Applied Physics 41:175405

Instability of Hydrostatically and Electrostatically Actuated Circular Microplates, Composite Structures 95:430–442.

Israelachvili, J. N. and Tabor, D. (1972) The Measurement of Van Der Waals Dispersion Forces in the Range 1.5 to 130 nm. Proceeding of the Royal Society A 331 19-38

Klimchitskaya, G. .L, Mohideen, U., Mostepanenko, V. M. (2000) Casimir and van der Waals forces between two plates or a sphere (lens) above a plate made of real metals. Physical Review A 61:062107(12pp)

Koiter, W.T. (1964) Couple-stresses in the theory of elasticity: I and II, Proc. K. Ned. Akad. Wet. B 67 (1):17–44.

Kolpekwar, A., Kellen, C., Blanton, R.D. (1998) Fault model generation for MEMS, in: M. Laudon, B. Romanowicz (Eds.), Proceedings of the International Conference on Modeling and Simulation of Microsystems, Semiconductors, Sensors and Actuators, Computational Publications, Cambridge, MA, pp. 111–116.

Kong, S. (2013) Size effect on pull-in behavior of electrostatically actuated microbeams based on a modified couple stress theory. Applied Mathematical Modelling 37:7481–7488

Koochi, A. and Abadyan, M. (2011) Evaluating the Ability of Modified Adomian Decomposition Method to Simulate the Instability of Freestanding Carbon Nanotube: Comparison with Conventional Decomposition Method. Journal of Applied Sciences 11 (19):3421-3428.

Lam, D.C.C., Yang, F., Chong, A.C.M., Wang, J., Tong, P. (2003) Experiments and theory in strain gradient elasticity. Journal of the Mechanics and Physics of Solids 51:1477-1508.

Lifshitz, E.M. (1956) The Theory of Molecular Attractive Force Between Solids. Soviet physics JETP 2:73-83.

Lin W. H. and Zhao Y. P. (2003) Dynamic behavior of nanoscale electrostatic actuators, Chinese Physics Letters 20:2070–2073.

McElhaney, K.W., Valssak, J.J., Nix, W.D. (1998) Determination of indenter tip geometry and indentation contact area for depth-sensing indentation experiments. J. Mater. Res.13:1300-1306

Mindlin, R. D. (1964) Micro-structure in linear elasticity, Arch. Rational Mech. Analys. 16:51-78.

Mindlin, R. D., Eshel, N. N. (1968) On First Strain-Gradient theories in linear elasticity, Int. J. Solid Struct. 4:109-124

Mindlin, R.D. and Tiersten, H.F. (1962) Effects of couple-stresses in linear elasticity. Archive for Rational Mechanics and Analysis 11:415–448

Moghimi Zand, M., Ahmadian, M.T., Rashidian, B. (2010) Dynamic pull-in instability of electrostatically actuated beams incorporating Casimir and van der Waals forces. Proceedings of the Institution of Mechanical Engineers - Part C: Mechanical Engineering Science 224:2037-2047.

Mohammadi M., Goodarzi M., Farajpour A., Ghayour M. (2013) Influence of in-plane pre-load on the vibration frequency of circular graphene sheet via nonlocal continuum theory, Composites: Part B 51: 121–129.

Mohammadi M., Goodarzi M., Ghayour M., Alivand S. (2012) Small Scale Effect on the Vibration of Orthotropic Plates Embedded in an Elastic Medium and Under Biaxial In-plane Pre-load Via Nonlocal Elasticity Theory, Journal of Solid Mechanics 4: 128- 143.

Mohammadi, V., Ansari, R., Faghih Shojaei, M., Gholami, R., Sahmani, S. (2013) Size-dependent dynamic pull-in instability of hydrostatically and electrostatically actuated circular microplates, Nonlinear Dynamics 73:1515-1526.

Moosavi H., Mohammadi M., Farajpour A., Shahidi S. H. (2011) Vibration analysis of nanorings using nonlocal continuum mechanics and shear deformable ring theory, Physica E 44: 135 –140.

Nix,W.D. and Gao, H. 1998. Indentation size effects in crystalline materials: A law for strain gradient plasticity. J. Mech. Phys. Solids 46:411-425

Noghrehabadi, A., Eslami, M., Ghalambaz, M. (2013) Influence of size effect and elastic boundary condition on the pull-in instability of nano-scale cantilever beams immersed in liquid electrolytes. International Journal of Non-Linear Mechanics 52:73–84.

Noghrehabadi, A., Tadi Beni, Y., Koochi, A., Kazemi, A. S., Yekrangi, A., Abadyan M., Noghrehabadi, M. (2011) Closed-form Approximations of the Pull-in Parameters and Stress Field of Electrostatic Cantilever Nanoactuators Considering van der Waals Attraction. Procedia Engineering 10: 3758-3764.

Rajabi, F., Ramezani, S. (2013) A nonlinear microbeam model based on strain gradient elasticity theory. Acta Mechanica Solida Sinica 26(1):21-34.

Ramezani, A., Alasty, A., Akbari, J. (2007) Closed-form solutions of the pull-in instability in nano-cantilevers under electrostatic and intermolecular surface forces. International Journal of Solids and Structures 44:4925–4941.

Ramezani, A., Alasty, A., Akbari, J. (2008) Analytical investigation and numerical verification of Casimir effect on electrostatic nano-cantilevers. Microsystem Technologies 14:145–157.

Reddy, J.N. (2007) Nonlocal theories for bending, buckling and vibration of beams, International Journal of Engineering Science 45:288–307

Rokni, H., Seethaler, R.J., Milani, A.S., Hashemi, S.H., Li, X.F. (2013)Analytical closed-form solutions for size-dependent static pull-in behavior in electrostatic micro-actuators via Fredholm integral equation. Sensors and Actuators A 190:32– 43.

Rotkin, S. V. (2002) Analytical calculations for nanoscale electromechanical systems. Electromechanical Society Proceeding 6:90–97.

Sadeghian, H., Yang, C. K., Goosen, J.F.L., van der Drift, E., Bossche, A., French, P.J., and Van Keulen, F. (2009) Characterizing size-dependent effective elastic modulus of silicon nanocantilevers using electrostatic pull-in instability. Applied Physics Letters 94 (22):221903 - 221903-3.

Soroush, R., Koochi, A., Kazemi, A. S., Abadyan, M. (2012) Modeling the effect of van der Waals attraction on the instability of electrostatic Cantilever and Doubly-supported Nano-beams using Modified Adomian Method. International Journal of Structural Stability and Dynamics 12(5): 1250036 (18 pp).

Stolken, J.S. and Evans, A.G, (1998) A microbend test method for measuring the plasticity length scale. Acta Materialia 46(14):5109-5115

Sundararajan, S. and Bhushan, B. (2002) Development of AFM-based techniques to measure mechanical properties of nanoscale structures. Sensors Actuators A 101:338-351.

Tadi Beni, Y., Abadyan, M., Noghrehabadi, A. (2011) Investigation of Size Effect on the Pull-in Instability of Beam type NEMS under van der Waals Attraction, Procedia Engineering 10:1718–1723.

Tadi Beni, Y., Koochi, A., Abadyan, M. (2011) Theoretical study of the effect of Casimir force, elastic boundary conditions and size dependency on the pull-in instability of beam-type NEMS. Physica E 43:979-988.

Tadi Beni, Y., Vahdati, A.R., Abadyan, M. (2013) Using ALE-FEM to simulate the instability of beam-type nano-actuator in the presence of electrostatic field and dispersion forces. IJSTM, Transaction of Mechanical Engineering 37:1-9.

Toupin, R. A. (1962) Elastic materials with couple stresses, Arch. Rational Mech. Analys. 11: 385-414.

Wang, B., Zhou, S., Zhao, J., Chen, X. (2011) Pull-in Instability Analysis of Electrostatically Actuated Microplate with Rectangular Shape. International Journal of Precision Engineering and Manufacturing 12:1085-1094.

Wang, B., Zhou, S., Zhao, J., Chen, X. (2011) Size-dependent pull-in instability of electrostatically actuated microbeam-based MEMS. Journal of Micromechanics and Microengineering 21:027001.

Wang, B., Zhou, S., Zhao, J., Chen, X. (2012) Pull-in instability of circular plate mems: a new model based on strain gradient elasticity theory. International Journal of Applied Mathematics 4:1250003.

Wang, W., Huang, Y., Hsia, K.J., Hu, K.X., Chandra, A. (2003). A study of microbend test by strain gradient plasticity. Int. J. Plasticity 19:365–382.

Wilson, C.J. and Beck, P.A. (1996) Fracture testing of bulk silicon microcantilever beams subjected to a side load. Journal of Microelectromechanical Systems 5:142-150.

Yang, F., Chong, A.C.M., Lam, D.C.C., Tong, P. (2002) Couple stress based strain gradient theory for elasticity. International Journal of Solids and Structures 39:2731–2743.

Yin, L., Qian, Wang, Q. L. (2011) Size effect on the static behavior of electrostatically actuated microbeams. Acta Mechanica Sinica 27:445–451.

Zhang, J. and Fu, Y. (2012) Pull-in analysis of electrically actuated viscoelastic microbeams based on a modified couple stress theory. Meccanica 47:1649-1658.

Zhang, L., Golod, S.V., Deckardt, E., Prinz, V., Grützmacher, D. (2004) Free-standing Si/SiGe micro- and nano-objects. Physica E 23(3):280-284.